ANL Mixed Potential Model For Used Fuel Degradation: Application to Argillite and Crystalline Rock Environments

Used Fuel Disposition

Prepared for
U.S. Department of Energy
Used Fuel Disposition Campaign

James Jerden[1]
Kurt E. Frey[2]
Jacqueline M. Copple[1]
William Ebert[1]
Argonne National Laboratory
University of Notre Dame

July 14, 2014
FCRD-UFD-2014-000490

This work was supported by the US Department of Energy, Office of Nuclear Energy. The report was prepared at Argonne National Laboratory as part of the Used Fuel Disposition (UFD) Campaign.

SUMMARY

This work is being performed as part of the DOE NE Used Fuel Disposition (UFD) Campaign Argillite and Crystalline Rock work packages: FT-14AN080601 and FT-14AN080701. This document meets both the July 14, 2014 and August 15, 2014 milestones: M4FT-14AN0806011 and M4FT-AN0807011.

The main accomplishments for Argonne's FY2014 work on the Mixed Potential Model (MPM) development project were as follows:

- Added a working noble metal particle (epsilon phase) domain on fuel surface to account for the protective hydrogen effect.
- Incorporated the radiolysis model subroutine in MPM (in collaboration with PNNL)
- Performed systematic sensitivity runs to identify and quantify the processes that affect the fuel dissolution rate.
- Compared sensitivity results with available experimental data (ongoing)
- Developed a research priority list based on results from sensitivity study and comparison with experimental results

The key observation to come out of the MPM sensitivity studies was that the set of coupled electrochemical reactions that comprise the model can be used to quantify the effectiveness of hydrogen within a breached canister to effectively shut down the radiolytic oxidative dissolution of the fuel. At sufficiently high hydrogen concentrations, fuel dissolution will only occur through the much slower chemical dissolution mechanism. This is consistent with experimental results from a number of repository programs (e.g., Shoesmith, 2008; Grambow and others, 2010) and with results from initial electrochemical tests performed in FY2013 as part of this study. The capacity to quantify the hydrogen effect in the used fuel degradation model will provide more realistic radionuclide source terms for use in PA.

The relative effects of temperature, dose rate (burnup), radiolysis, pH, carbonate complexation, ferrous iron and corrosion layer formation were also evaluated in the FY2014 sensitivity runs. All of these variables will influence the fuel degradation rate in distinct ways within argillite and crystalline rock, and other potential disposal environments. However, our sensitivity runs show that the hydrogen effect could be by far (up to four orders of magnitude greater, depending on the hydrogen concentration) the most dominant.

The MPM is uniquely suited to quantify the hydrogen effect on used fuel degradation because it explicitly accounts for all relevant interfacial redox reaction kinetics using fundamental electrochemical principles. This includes the impacts of phases present in the fuel, such as the catalytic effects of noble metal particles and the fuel surface itself, and other materials present in the disposal system that supply reactants or affect key redox reactions. The anoxic corrosion of steels present in the waste package is the main source of hydrogen in the waste package. The MPM was developed with the initial focus on reactions at the fuel surface, and the dissolved hydrogen concentration is currently a user-input value. To account for the hydrogen effect in long-term model runs, corrosion kinetics of steel components leading to hydrogen generation

needs to be incorporated into the model and coupled with fuel dissolution kinetics through the dissolved hydrogen concentration.

The current version of the MPM has proven effective for quantifying key processes affecting the rate of used fuel degradation; however, the implementation of MPM within a performance assessment model requires further model development and focused experimental work to provide data and quantify uncertainties in the existing database used to determine model parameter values representing disposal environments of interest. In order to take advantage of the work that has been done so far on the MPM, a number of needs have been identified:

- Incorporate the kinetics for hydrogen generation during the anoxic corrosion of steels into MPM as the source term for hydrogen.
- Perform focused electrochemical experiments with noble metal particle and lanthanide-doped UO_2 electrodes to determine parameter values needed to accurately model the effects of hydrogen, potential catalytic poisons such as bromide, and the pH and reaction temperature dependencies of fuel dissolution.
- Convert the MPM from MATLAB to Fortran to facilitate integration with PA codes (PFLOTRAN) (ongoing)
- Complete sensitivity runs to identify and assess inputs and outputs for integrating Fortran MPM into PA

CONTENTS

1. Objectives and Introduction

The high-level objective for this work is to develop a used fuel degradation model that:

- Calculates the dissolution rate of used fuel based on the corrosion potential and redox reaction currents of electrochemical reactions (most importantly the anodic reaction releasing UO_2^{2+} into solution, which is the fuel dissolution rate) that are established at the fuel/solution interface.
- Produces surface area-scalable results that can be used to define a fractional fuel degradation rate for performance assessment models.
- Accounts for interfacial redox reaction kinetics, radiolytic oxidants (H_2O_2), and the catalytic behavior of the noble metal particles (NMP) present within the fuel.
- Accounts for the evolution of fuel burnup and the related temperature and dose histories of the exposed fuel.

The objectives specifically addressed in FY2014 are shown in the context of previous and future work in Figure 1. Briefly, MPM V.1 represents the implementation of the model developed in Canada with modifications to facilitate including additional processes affecting fuel dissolution. Specifically, MPM V.2 includes separate UO_2 and NMP phases to model catalytic effects, a more sophisticated radiolysis model, and a modified diffusion model that facilitates calculations over long times. Other planned modifications include adding a steel corrosion module to quantify hydrogen generation, modifying the catalytic efficiency of NMP to account for the effects of catalytic poisons in the groundwater (e.g., bromide) and corrosion, and evolving the reactive surface area of the corroding fuel. This report focuses on the progress made during FY 2014 in the following areas:

- Integrating the MPM with the Radiolysis Model (RM) developed at PNNL (e.g., Buck et al., 2013).
- Updating the MPM parameter database based on an ongoing literature review.
- Performing sensitivity runs with the updated MPM.
- Translating MPM (with RM subroutine) to Fortran 2003 to facilitate integration with performance assessment models.

A generalization of the envisioned relationships between the MPM and the generic performance assessment models for the argillite and crystalline rock disposal concepts is shown in Figure 2. Updates to the parameter database and the information exchange between the MPM and PA models summarized in Figure 2 are discussed in this report.

Part of the proposed scope of FY2015 will be to begin the process of actually integrating the MPM into the generic performance assessment models for argillite and crystalline repositories. Specifically the MPM will be used to calculate the dissolution rate or fractional degradation rate of used fuel to provide source terms for radionuclides released from a breached waste package. Work to extend the MPM to include the chemical and redox effects of canister corrosion (primarily the hydrogen source term in the waste package) will be coordinated with container breaching models being developed in other UFD activities. The extensive parameter database used by the MPM V2 (presented below) makes it applicable to a wide range of geochemical

settings (e.g., Tables 1 and 2); however, more experimental data are required to reduce uncertainties in key functionalities such as the pH and temperature dependencies of rate constants.

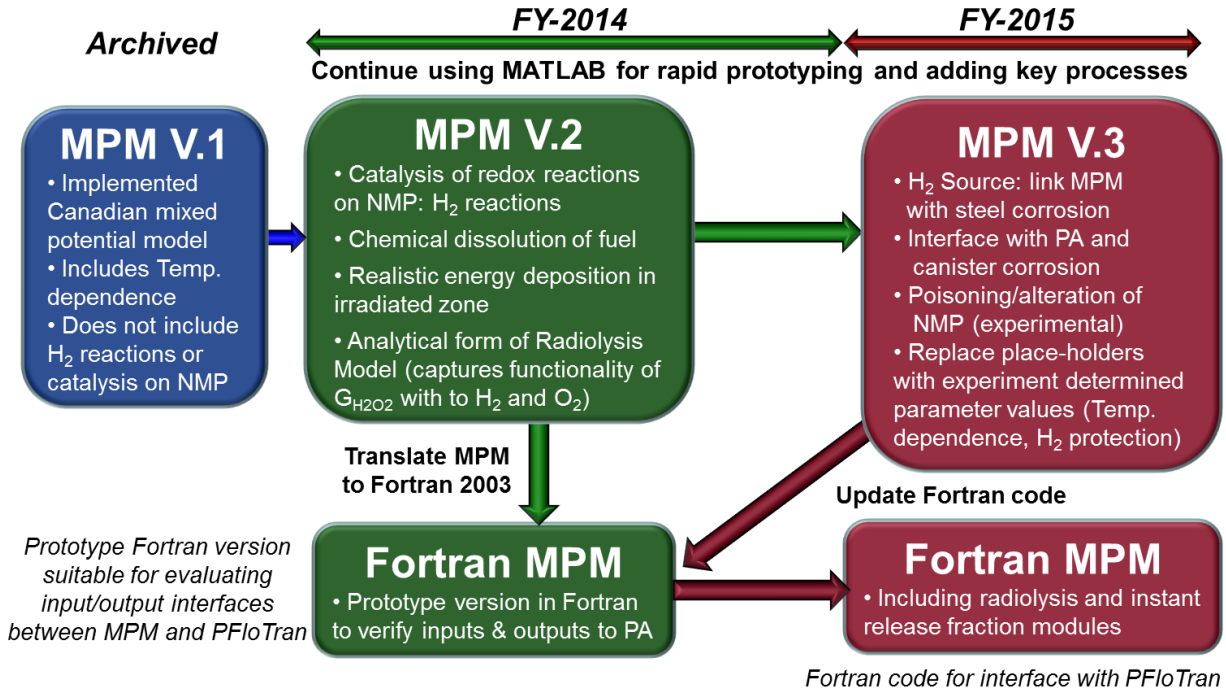

Figure 1. Schematic flow diagram highlighting progress made in the development of the MPM and future priorities based on sensitivity results from MPM V.2.

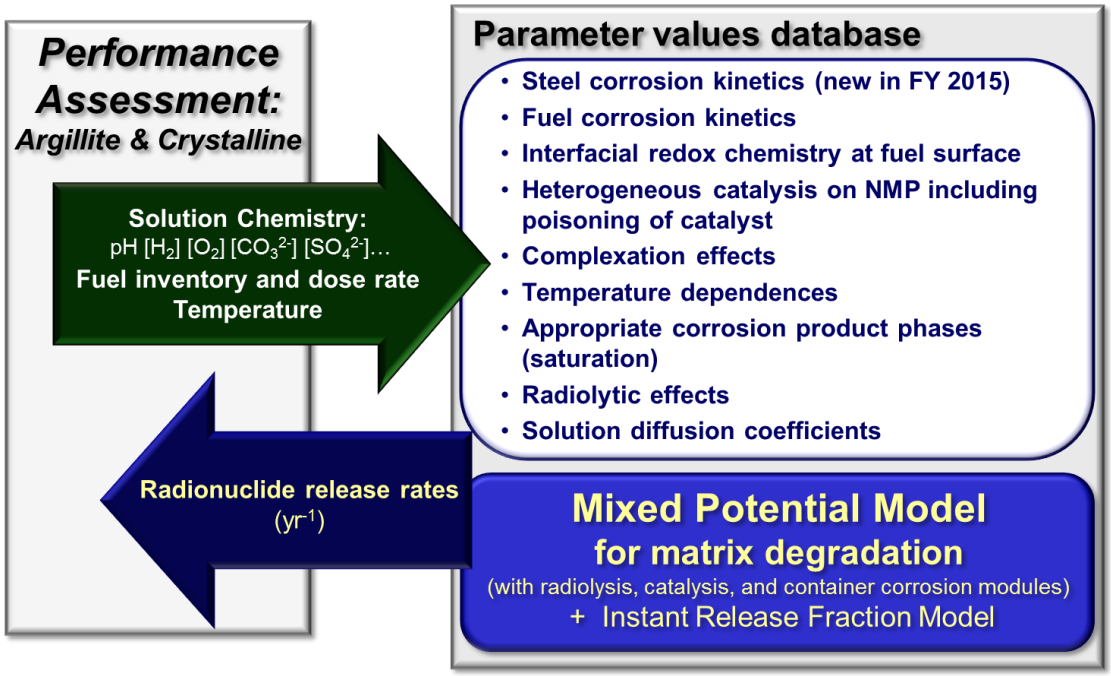

Figure 2. Schematic flow diagram showing relationships between the MPM and the generic performance assessment models.

1.1 Summary of Argillite and Crystalline Rock Repository Concepts

Clayrock/shale (here synonymous with argillite) bedrock formations are recognized as promising repository host rocks. For example, Callovo-Oxfordian formations at Bure France, the Boom Clay at Mol Belgium, the Boda formations at Mecsek Hungary, the Opalinus Clay at Mont Terri Switzerland, the Oxford Clay in the UK and the Queenston formation in Canada (list from Gaucher et al., 2009). Due to their low permeability, it is difficult to extract undisturbed water samples from clayrock formations; therefore, modeling techniques base on equilibrium with dominant mineral assemblages have been developed (e.g., Gaucher et al., 2009).

Table 1 shows a typical modeled clayrock/shale pore water composition and a measured pore water composition from The Callovo-Oxfordian in France (Vinsot et al., 2008).

Table 1. Measured and modeled pore water compositions from a clayrock or argillite formation. The model assumes that the water is in equilibrium with the mineral assemblage illite-calcite-dolomite-iron chlorite-quartz-pyrite–celesite. The measured composition is from the Callovo-Oxfordian formations in France.

	Model (Gaucher et al., 2009)	Measured (Vinsot et al., 2008)
pH	7.1	7.2
Eh_{SHE} (mV)	-163	-199
	(moles/kg)	(moles/kg)
Inorganic C	2.19E-3	4.2E-3
Cl	3.01E-2	4.1E-2
S	3.39E-2	1.9E-2
Na	3.21E-2	5.6E-2
K	7.09E-3	9.0E-4
Ca	1.49E-2	7.6E-3
Mg	1.41E-2	5.9E-3
Sr	1.12E-3	2.5E-4
Si	9.41E-5	1.4E-4
Al	7.39E-9	----
Fe	2.14E-4	1.5E-5

These values can be used to place the MPM V2 model runs within the contexts of the geologic environments in question. Crystalline shield sites that have been identified as promising as repository settings include rock units in Canada, Finland and Sweden. Examples of crystalline rock groundwater chemistries are shown in Table 2.

Table 2. Modeled and measured pore water compositions from crystalline rock units (compiled by Guimera et al., 2006). The model is for a fracture hosted groundwater after 5,000 years of a deglaciation period at repository depth (for discussion see Guimerà et al., 2006).

Components	Forsmark groundwater	Grimsel groundwater	5,000 year old Forsmark water (modeled)
pH	7.0	9.6	9.8
Eh_{SHE} (mV)	-143	-200	-240
	(moles/L)	(moles/L)	(moles/L)
HCO_3^-	1.77E-3	4.50E-4	9.28E-5
Cl	1.53E-1	1.60E-4	4.04E-4
S	6.80E-3	6.10E-5	----
Na	8.88E-2	6.90E-4	6.90E-4
K	8.75E-5	5.00E-6	3.18E-4
Ca	2.33E-2	1.40E-4	2.17E-4
Mg	9.30E-3	6.20E-7	6.20E-7
Si	1.85E-4	2.50E-4	5.60E-4
Br	2.98E-4	3.80E-7	3.80E-7
Fe	3.31E-5	3.00E-9	2.91E-7

As will be discussed below, the chemical properties of the groundwater examples shown in Tables 1 and 2 that will influence the MPM fuel dissolution rate calculations are the pH, Eh, dissolved carbonate and dissolved iron. Chloride and bromide are also important species because they are radiolytically active. It is expected that future versions of the MPM will account for radiolytically active halides after planned experiments to quantify their effects on the fuel dissolution rate.

The MPM V2 sensitivity runs discussed in Section 3 below account for the full ranges of groundwater compositions expected from different argillaceous and crystalline repository environments.

1.2 Mixed Potential Model Process Overview

As shown in Figure 1, the Argonne MPM was developed based on the Canadian-mixed potential model for UO_2 fuel dissolution of King and Kolar, 2003 and was implemented using the numerical computing environment and programming language MATLAB (Jerden et al., 2013). The MPM is a 1-dimensional reaction-diffusion model that accounts for the following processes:

- Rate of oxidative dissolution of the fuel matrix U(VI) as determined by interfacial redox reaction kinetics (quantified as a function of the corrosion potential) occurring at the multiphase fuel surface (phases include UO_2 and the noble metal fission product alloy phase (NMP), often referred to as the epsilon phase).
- Chemical (solubility-based) dissolution of the fuel matrix U(IV).
- Complexation of dissolved uranium by carbonate near the fuel surface and in the bulk solution.

- Production of hydrogen peroxide (which is the dominant fuel oxidant in anoxic repository environments) by alpha-radiolysis.
- Diffusion of reactants and products in the groundwater towards and away from the reacting fuel surface.
- Precipitation and dissolution of a U–bearing corrosion product layer on the fuel surface.
- Diffusion of reactants and products through the porous and tortuous corrosion product layer covering the reacting fuel surface.
- Arrhenius-type temperature dependence for all interfacial and bulk reactions.

In the MPM, the fuel degradation rate is calculated using mixed potential theory to account for all relevant redox reactions at the fuel surface, including those involving oxidants produced by solution radiolysis. Because the MPM is based on fundamental chemical and electrochemical principles, it is flexible enough to be applied to the full range of repository environments and conditions.

Of particular interest is the surface chemical properties of the NMP, which have been shown to catalyze redox reactions at the fuel/solution interface (e.g., Broczkowski et al., 2005, Shoesmith, 2008, Trummer, et al., 2009, Cui et al., 2010). These studies show that the degradation rate of the used fuel may be dramatically affected if dissolved hydrogen is present. Therefore, this process was incorporated into the MPM V2 using user-input hydrogen concentrations (Jerden et al., 2013).

In FY2014, the MPM V2 with the catalytic NMP domain was run for a number of conditions to determine the relative effects of key variables such as temperature, dose rate, and solution chemistry. As discussed below, the most important process in terms of fuel dissolution rate is the reaction of hydrogen at the NMP domains. The main source of hydrogen in the repository near field and waste package will be as a by-product of the anoxic corrosion of steel. This process and its relationships to the MPM calculated used fuel degradation rate are shown in Figure 3. Figure 3a illustrates the abundance of steel surrounding the fuel in a generic waste package. Figure 3b shows the chemical and redox couples between the fuel dissolution (i.e., the reaction releasing UO_2^{2+} into the solution between corroding steel and the fuel). The reaction releasing UO_2^{2+} into solution is the key reaction modeled by the MPM and is defined as the fuel dissolution rate

$$UO_2 + H_2O_2 = UO_2^{2+} + 2\ OH^-. \quad (1)$$

The MPM is designed to quantify the effects of other reactions and processes on the kinetics of that reaction through chemical and electrochemical couples. The diagram in Figure 3c shows the catalyzed oxidation of hydrogen on the NMP surface and the transfer of electrons from NMP sites to the fuel matrix are coupled chemically through the dissolved hydrogen concentration. The electrical coupling between NMP and fuel grains establishes a galvanic link that effectively protects the fuel from oxidative dissolution by mitigating the reaction in Equation 1. The poisoning of NMP shown on the right side represents catalytic deactivation due to the formation of surface coatings and corrosion. The kinetics of the steel oxidation to release H_2 and the effects of poisoning of NMP remain to be included in the MPM; this is planned for FY 2015.

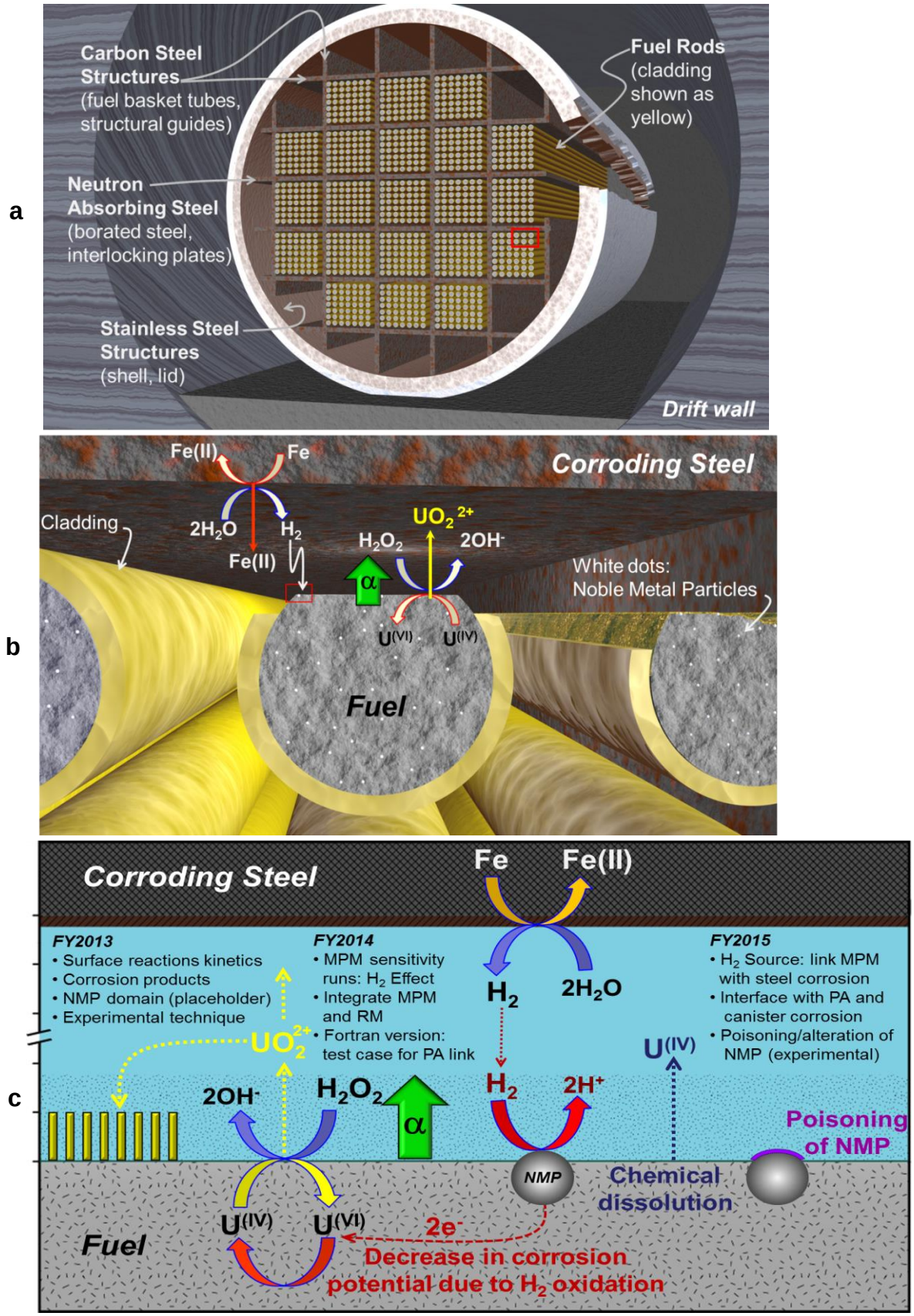

Figure 3. Conceptual diagrams of a used fuel waste package (a), exposed fuel (b), and a summary of the key interfacial processes that determine the overall degradation rate highlighting when each process was/will be incorporated into the MPM (c).

2. Updated MPM Parameter Database for Argillite and Crystalline Repository Environments

Tables 3 – 7 show the MPM parameter database that has been updated based on recent literature and used in sensitivity runs discussed in below. Although there remain quite a few estimated values that require experimental evaluation to quantify model uncertainties, the sensitivity runs yield important information about the relative (order of magnitude) effects that different variables have on the predicted fuel dissolution rate. The results can be used to prioritize which parameters are experimentally verified.

The extensiveness of the MPM parameter database makes it possible to use the model to calculate used fuel dissolution rates over a wide range of geochemical and electrochemical conditions. For example, the model accounts for the range of temperature, pH and carbonate concentrations anticipated in both argillite and crystalline rock repositories (e.g., Tables 1 and 2).

Table 3. Parameter and variable inputs used for in sensitivity runs with MPM V2.

Variables set by user (these will ultimately be inputs from other PA models)	**Range of values used in Sensitivity runs**	**Notes**
Temperature	25 ^{o}C to 200 ^{o}C	The evolution of the waste form temperature will be the output of other models accounting for burnup, fuel age, repository design, etc.
Dose rate	1 – 500 rad/s	Dose evolution will also be the output of other models accounting for fuel burnup and age.
Environmental concentration of dissolved oxygen	Zero to millimolar	This key variable will be determined by a number of interdependent kinetic processes within the waste package and near-field, but the dominant buffer may be the geologic environment: Argillite vs. Crystalline Rock.
Environmental concentration of dissolved carbonate	Zero to millimolar	This is a key variable determined by specifics of the geologic environment: Argillite vs. Crystalline Rock.
Environmental concentration of dissolved ferrous iron	Zero to millimolar	This key variable will be determined by a number of interdependent kinetic processes within the waste package and near-field, but the dominant source will be corroding steel components.
Environmental concentration of dissolved hydrogen	Zero to millimolar	This key variable (the most important for the present work) will also be determined by a number of interdependent kinetic processes within the waste package and near-field, but the dominant source will be anoxic corrosion of steel components.

pH	4 to 9.5	The effect of pH is incorporated into the MPM V2 by modifying the rate constants for fuel dissolution (Table 4) based on the experimental results of Torrero et al., 1997 which yield: r (mol/m^2s) = 3.5E-8$[H^+]^{0.37}$ for pH 3.0 to 6.7 and r (mol/m^2s) = 3.5E-8ror pH values greater than 6.7. *Note*: groundwaters in Argillite and Crystalline environments are anticipated to have pH > 6.7 (e.g., Tables 1 and 2).
Space and Time Parameters		
Length of diffusion grid in model	3 mm	Arbitrary, can be changed by user to represent system of interest.
Number of calculation nodes (points) in diffusion grid	200	Arbitrary, can be changed by user to optimize calculation efficiency.
Duration of simulation	100,000 years	Arbitrary, can be changed by user to represent duration of interest.
Radiolysis Parameters		
Alpha-particle penetration depth	35 micrometers	The basis for this value was re-examined in FY 2014, but remains unchanged (confirmed).See section 2.1 for discussion.
Generation value for H_2O_2	Calculated by new Radiolysis Model subroutine	In MPM V2, this value varies depending on the dose rate and dissolved concentrations of O_2 and H_2 within the irradiation zone (see Section 2.2 below)
Physical Interfacial Parameters		
Surface coverage of NMP	Zero to 1%	Based on qualitative examination of photomicrographs of spent fuels of different burnups e.g., Tsai, 2003.
Resistance between UO_2 and NMP domains	Constant 1.0E-3 V/Amp	Assumed that fuel and NMP are electrically well-coupled
Porosity of schoepite corrosion layer	50%	Reasonable assumption based on qualitative assessment of photomicrographs of schoepite layers e.g., Finch and Ewing, 1992.
Tortuosity factor of schoepite corrosion layer	0.1	Reasonable assumption based on analogy of schoepite layer with compacted clay (King and Kolar, 2003)

Table 4. Rate constants for all relevant reactions and their associated activation energies used in MPM V2. The far right column provides notes on recent updates based on our on-going literature survey.

Reaction	**Rate Constant** (mol/m^2 s)	**Activation energy** (J/mole)	**Updates based on literature review**
Fuel Dissolution Reaction			
$UO_2^{fuel} \rightarrow UO_2^{2+} + 2e^-$	5.00E-08	6.00E+04	Zeroth-order electrochemical rate constant for the irreversible oxidation of UO_2 from King and Kolar, 2003.
$UO_2^{fuel} + 2CO_3^{2-} \rightarrow UO_2(CO_3)_2^{2-} + 2e^-$	1.30E-08	6.00E+04	Electrochemical rate constant for the irreversible oxidation of UO_2 in carbonate solution from King and Kolar, 2003. (the reaction order with respect to carbonate is m = 0.66).
$UO_2^{fuel} \rightarrow UO_2(aq)$	8.60E-12	6.00E+04	Based on solubility of UO_2 in reducing conditions. Calculated using GWB and YMP data0 R5 thermodynamic database.
Reactions at Fuel Surface	(m/s)	(J/mole)	
$H_2O_2 \rightarrow O_2 + 2H^+ + 2e^-$	7.40E-08	6.00E+04	1st-order electrochemical rate constant for irreversible oxidation of H_2O_2 on UO_2 estimated based on assumption that, at a potential of 0.08 VSCE, the oxidation and reduction rates of H_2O_2 on UO_2 are equal and that the Tafel slopes are identical: from King and Kolar, 2003.
$H_2O_2 + 2e^- \rightarrow 2OH^-$	1.20E-12	6.00E+04	1st-order electrochemical rate constant for irreversible reduction of H_2O_2 on UO_2: from King and Kolar, 2003.
$O_2 + 2H_2O + 4e^- \rightarrow 4OH^-$	1.40E-12	6.00E+04	1st-order electrochemical rate constant for irreversible reduction of O_2 on UO_2: from King and Kolar, 2003.
Reaction at NMP surface	(m/s)	(J/mole)	
$H_2O_2 \rightarrow O_2 + 2H^+ + 2e^-$	7.40E-07	6.00E+04	1st-order electrochemical rate constant for irreversible oxidation of H_2O_2 on NMP catalyst, assumed to be one order of magnitude faster than on oxide - needs experimental evaluation.

$H_2O_2 + 2e^- \rightarrow 2OH^-$	1.20E-11	6.00E+04	1st-order electrochemical rate constant for irreversible reduction of H_2O_2 on NMP catalyst: assumed to be one order of magnitude faster than on oxide - needs experimental evaluation.
$O_2 + 2H_2O + 4e^- \rightarrow 4OH^-$	1.40E-11	6.00E+04	1st-order electrochemical rate constant for irreversible reduction of O_2 on NMP catalyst: assumed to be one order of magnitude faster than on oxide - needs experimental evaluation.
$H_2 \rightarrow 2H^+ + 2e^-$	5.00E-04	6.00E+04	1st-order electrochemical rate constant for irreversible oxidation of H_2 on NMP catalyst: based on data for Pt-Ru catalyst (Uchida et al., 2009) - needs experimental evaluation.
Corrosion Layer Reactions	(/s)	(J/mole)	
$UO_2^{2+} + 2H_2O \rightarrow UO_3{:}2H_2O + 2H$	1.00E-03	6.00E+04	Estimate based on residence time of UO_2^{2+} in supersaturated solution - needs experimental/literature evaluation. Rate law from King and Kolar, 2003: $1.0E\text{-}3*\exp(6.0E4*dT)/(2.4*[UO_2^{2+}]_{saturation})^4$.
$UO_2(CO_3)_2^{2-} + 2H_2O \rightarrow UO_3{:}H_2O + 2CO_3^{2-} + 2H^+$	1.00E-04	6.00E+04	Estimate based on residence time of UO_2^{2+} in supersaturated solution containing carbonate - needs experimental/literature evaluation. Rate law from King and Kolar, 2003: $1.0E\text{-}4*\exp(6.0E4*dT)/(2.4*[UO_2(CO_3)_2^{2-}]_{saturation})^4$.
$UO_3{:}H_2O + 2CO_3^{2-} + 2H^+ \rightarrow UO_2(CO_3)_2^{2-} + 2H_2O$	6.30E-12	6.00E+04	Based on data for dissolution of soddyite in carbonate solution: from King et al., 2001.
Key Bulk Reactions	(/s)	(J/mole)	
$H_2O_2 \rightarrow H_2O + 0.5O_2$	4.50E-07	6.00E+04	Personal communication with Rick Wittman of PNNL on 3/12/2014, the overall reaction rate constant comes from runs using the PNNL Radiolysis model which uses rate constants from Pastina and Laverne, 2001.
	(m/mol s)	(J/mole)	
$O_2 + 4Fe^{2+} + 8OH^- \rightarrow 4H_2O + 2Fe_2O_3$	5.90E-01	6.00E+04	Rate is highly pH dependent below 8.0. Derived from experimental data at pH = 8.7 by King and Kolar, 2003.
$H_2O_2 + 2Fe^{2+} + 4OH^- \rightarrow 3H_2O + Fe_2O_3$	6.90E-01	4.20E+04	From King and Kolar, 2003, notes that pH dependence unknown - needs experimental evaluation.
$UO_2^{2+} + 2Fe^{2+} + 6OH^- \rightarrow UO_2 + 3H_2O + Fe_2O_3$	1.00E-02	6.00E+04	Assumed value based on similar redox reactions, from King and Kolar, 2003.

$UO_2(CO_3)_2^{2-} + 2Fe^{2+} + 6OH^- \rightarrow UO_2 + 2CO_3^{2-} + 3H_2O + Fe_2O_3$	1.00E-03	6.00E+04	Assumed value based on similar redox reactions, from From King and Kolar, 2003.

Table 5. Electrochemical parameters for all relevant reactions and their associated temperature dependence used in MPM V2. The far right column provides notes on recent updates based on our on-going literature survey.

Reactions	**Charge Transfer Coefficient**	**Standard Potential ($Volts_{SCE}$)**	**Temperature Dependence ($Volts_{SCE}/K$)**	**Updates based on literature review**
Fuel Dissolution				
$UO_2^{fuel} \rightarrow UO_2^{2+} + 2e^-$	9.60E-01	0.169	-2.48E-04	From King and Kolar, 2003
$UO_2^{fuel} + 2CO_3^{2-} \rightarrow UO_2(CO_3)_2^{2-} + 2e^-$	8.20E-01	-0.173	2.10E-03	From King and Kolar, 2003
Reactions at Fuel Surface				
$H_2O_2 \rightarrow O_2 + 2H^+ + 2e^-$	4.10E-01	-0.121	-9.93E-04	From King and Kolar, 2003
$H_2O_2 + 2e^- \rightarrow 2OH^-$	4.10E-01	-0.973	-6.98E-04	From King and Kolar, 2003
$O_2 + 2H_2O + 4e^- \rightarrow 4OH^-$	5.00E-01	-0.426	-1.23E-04	From King and Kolar, 2003
Reaction at NMP surface				
$H_2O_2 \rightarrow O_2 + 2H^+ + 2e^-$	4.10E-01	-0.121	-9.93E-04	Assumed to be equal to values on UO_2 surface - needs experimental evaluation.
$H_2O_2 + 2e^- \rightarrow 2OH^-$	4.10E-01	-0.973	-6.98E-04	Assumed to be equal to values on UO_2 surface - needs experimental evaluation.
$O_2 + 2H_2O + 4e^- \rightarrow 4OH^-$	5.00E-01	-0.426	-1.23E-04	Assumed to be equal to values on UO_2 surface - needs experimental evaluation.
$H_2 \rightarrow 2H^+ + 2e^-$	1	-0.421	0	Standard potential from Lide, R.D. (Ed.), 1999. Handbook of Chemistry and Physics, 80th ed. Charge transfer coefficient and temperature dependence need experimental evaluation.

Table 6. Diffusion coefficients and associated temperature dependence used in MPM V2. The far right column provides notes on recent updates based on our on-going literature survey.

Species	**Diffusion coefficient** (cm^2/s)	**Activation energy** (J/mole)	**Updates based on literature review**
UO_2^{2+}	7.66E-10	1.50E+04	Changed from 5.0E-10 (estimate King et al., 2001) based on Kerisit and Liu, 2010.
$UO_2(CO_3)_2^{2-}$	6.67E-10	1.50E+04	Changed from 5.0E-10 (estimate King et al., 2001) based on Kerisit and Liu, 2010.
$U(IV)O_2(aq)$	5.52E-10	1.50E+04	Assumed to be neutral species and set equal to neutral $UO_2CO_3(aq)$ from Kerisit and Liu, 2010.
CO_3^{2-}	8.12E-10	1.50E+04	Changed from 5.0E-10 (estimate King et al., 2001) based on Kerisit and Liu, 2010.
O_2	1.70E-09	1.50E+04	No change: from From King and Kolar, 2003.
H_2O_2	1.70E-09	1.50E+04	No change: from From King and Kolar, 2003.
Fe^{2+}	7.19E-10	1.50E+04	Added from Lide, R.D. (Ed.), 1999. Handbook of Chemistry and Physics, 80th ed.
H_2	5.00E-09	1.50E+04	Added from Macpherson and Unwin, 1997.

Table 7. Saturation concentrations and associated temperature dependence used in MPM V2. The far right column provides notes on recent updates based on our on-going literature survey.

Species	**Saturation Concentration** ($mole/m^3$)	**Activation energy** (J/mole)	**Updates based on literature review**
UO_2^{2+}	3.00E-02	-6.00E+04	Changed from 3.2E-2 $mole/m^3$ based on GWB runs using YMP data0 R5 equilibrium constant database. The negative activation energy reflects the observations of Murphy and Codell (1999) that common uranyl minerals exhibit retrograde solubility.
$UO_2(CO_3)_2^{2-}$	9.00E-02	-6.00E+04	Changed from $5.12(mol/cm^3)^{0.34}$ $mole/m^3$ based on GWB runs using YMP data0 R5 equilibrium constant database. The negative activation energy reflects the observations of Murphy and Codell (1999) that common uranyl minerals exhibit retrograde solubility
Fe^{++}	5.00E-02	6.00E+04	Changed from 3.2E-2 $mole/m^3$ based on GWB runs using YMP data0 R5 equilibrium constant database.

2.1 Alpha Particle Penetration Depth and Dose Rate Profile Used in MPM V2.

In the MPM, the primary oxidant driving the oxidative dissolution of the fuel is H_2O_2 formed by radiolysis and the width of the irradiated zone in which H_2O_2 is produced is of fundamental importance. (This was shown conceptually as the length of the green arrow labeled α in Figure 3c). Thus far, the Argonne MPM has used the value of 35 micrometers from the fuel surface as the width of the irradiated zone (also referred to as the alpha particle penetration depth), which is the value used in the Canadian mixed potential model of King and Kolar 2003. The basis for this value and its applicability was reexamined because the Canadian work assumed only CANDU fuel assemblies.

The width of the alpha penetration depth is determined by the energy of the alpha particles emitted from the fuel surface. The 2013 version of the well-established and validated code "The Stopping and Range of Ions in Matter" (SRIM, 2013) was used to determine the relationship between alpha particle energy and penetration depth in water (Figure 4). The results show that the alpha penetration depth can vary from between 35 μm for and alpha energy of around 5 MeV up to 55 μm for and alpha energy of 6.5 MeV. 5 – 6.5 MeV is the reasonable range of alpha energies emitted from used fuel.

Based on the used fuel energy spectra shown in Radulescu (2011), a reasonable argument can be made for using an energy value of 5 MeV for used fuel alpha particles. Furthermore, Radulescu (2011) show that the alpha energy spectra does not change dramatically with time; therefore it is also reasonable to use a constant alpha penetration depth of 35 μm throughout the duration of MPM simulations.

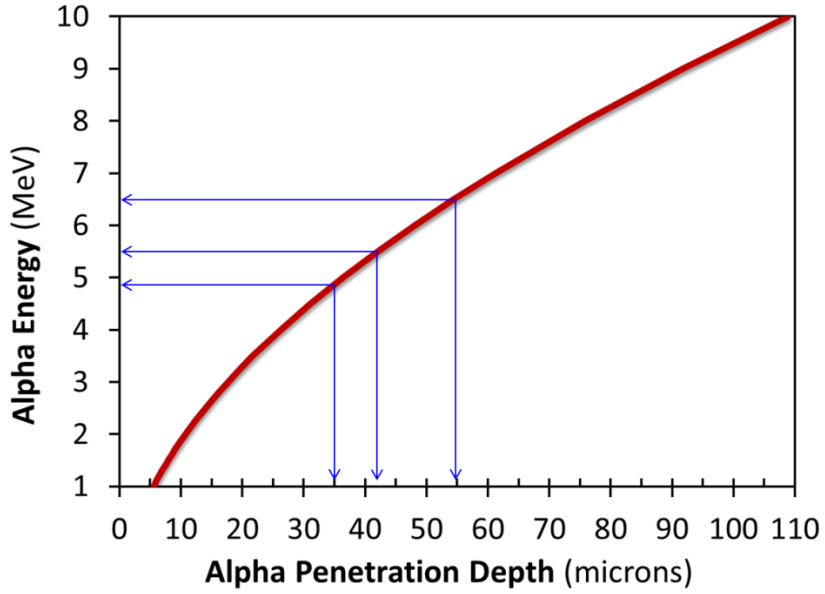

Figure 4. Alpha particle penetration depths vs. the alpha particle energy based on the stopping power of water, calculated using SRIM, 2013.

Another key physical quantity that determines the amount of radiolytic oxidants, and thus the local solution oxidative potential, is the dose rate within the alpha penetration zone. The earlier version of the MPM used a constant dose rate (step-function) across the entire 35 μm alpha irradiation zone. This assumption was conservative (produced the maximum amount of radiolytic oxidants) but was also physically unrealistic. This step function has been replaced in MPM V2 with an exponentially decreasing alpha dose rate within the alpha penetration zone (Figure 5). The analytical function shown the curve in Figure 5 was fit to the dependence measured by Nielsen and Jonsson, 2006 (blue circles).

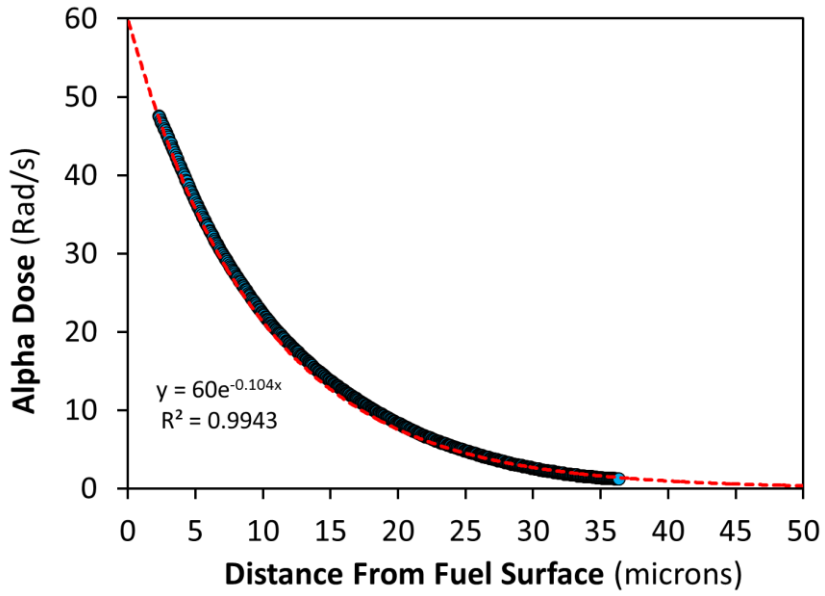

Figure 5. Alpha dose rate profile used in the MPM V2 (red line, $Y=60e^{-0.104x}$), which is a fit to the data points of Nielsen and Jonsson, 2006.

2.2 Incorporation of Radiolysis Model Analytical Function into MPM V2.

In January 2014, Rick Wittman and Edgar Buck of PNNL produced a straight forward analytical function that captures the functional dependence of the effective or conditional generation value of H_2O_2 (G_{H2O2}) on the local dissolved concentrations of H_2 and O_2. A description of the PNNL Radiolysis Model and the quantitative definition of the conditional G_{H2O2} can be found in Buck et al, 2013 and a forthcoming FY2014 PNNL report.

The function provided by PNNL was converted from Fortran to MATLAB and incorporated as a subroutine into the MPM V2 (Appendix 1). The radiolysis model function essentially replaces the constant G_{H2O2} value that had been used in MPM V1. The following relationship describes the basic equation for H_2O_2 production as a function of space and time used in MPM V2:

Molar yield of H_2O_2 (x,t) = $[G_{H2O2}](H_2,O_2)$ * [Dose Rate](x,t) * g(x)

The amount of H_2O_2 produced is determined as the product of G_{H2O2}, which is a function of local solution chemistry (radiolysis model subroutine), the dose rate, which varies in both time (as fuel decays) and space (see Figure 5), and a geometrical factor g(x). The geometrical factor accounts for how the diffusion of aqueous species is modified by the tortuosity of the uranyl corrosion layer (schoepite). The subroutine written in MATLAB code is shown in Appendix 1.

The topology of the radiolysis model function that determines G_{H2O2} in the MPM V2 is shown in Figure 6. The striking feature of this function is the precipitous decrease in the value of G_{H2O2} from around 1.0 (the value used in the previous MPM version) down to less than 0.1 for conditions of low dissolved O_2 and moderate to high concentrations of H_2. This feature is strongly dependent on the dose rate, as shown in the plots at the bottom Figure 6. The impact this G_{H2O2} "cliff" on the dissolution rate of used fuel calculated by the MPM V2 has been explored as part of the sensitivity runs (discussed in Section 3.0 below).

Sensitivity runs show that even at a low starting $[O_2]$ = 1.0E-9 moles/L, the dissolved concentration of O_2 rarely drops below 1.0E-7 moles/L. This is due to the production of O_2 as H_2O_2 decomposes at the fuel surface by the reaction $H_2O_2 \rightarrow O_2 + 2H^+ + 2e^-$.

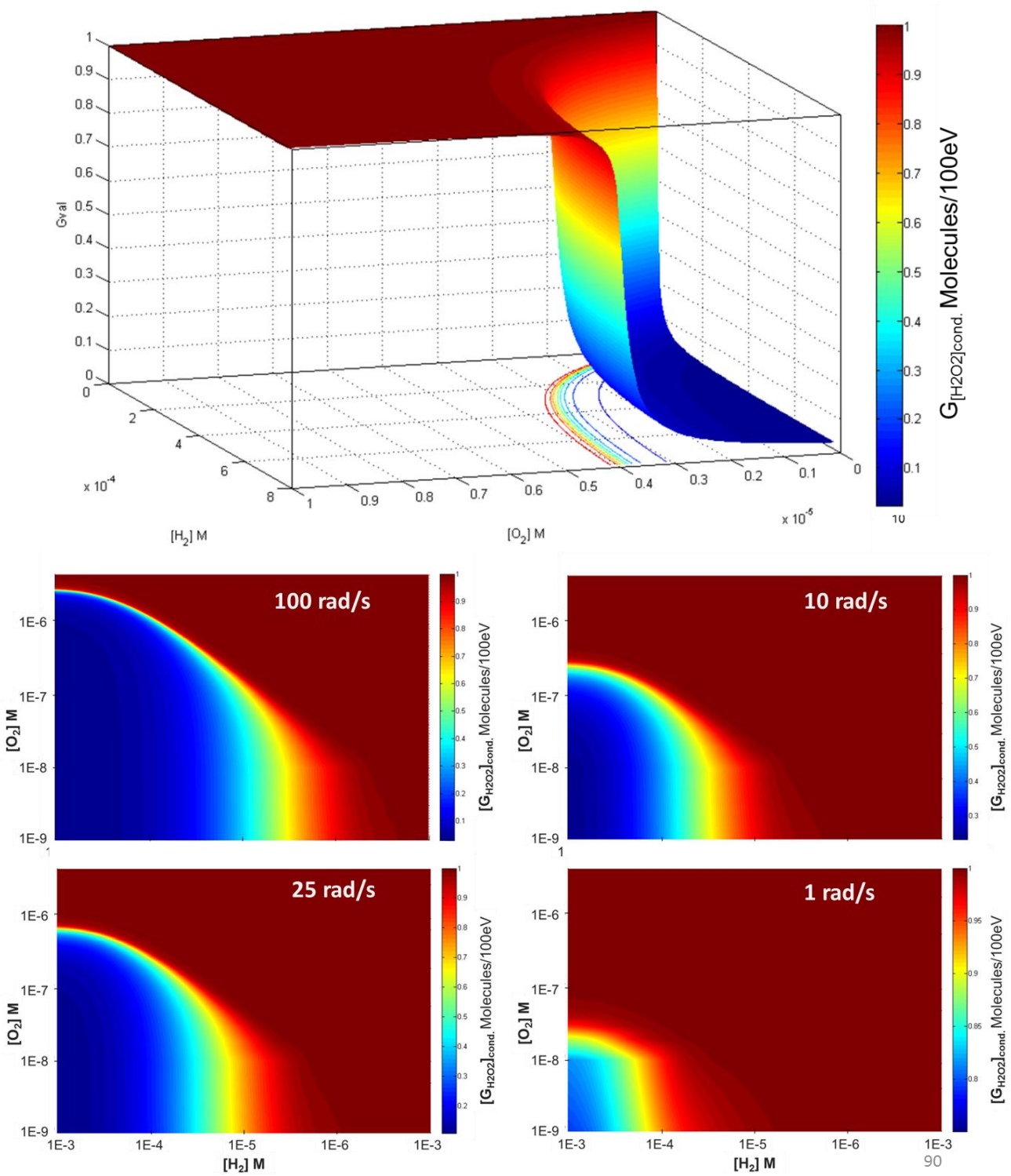

Figure 6. Topology of the analytical function that comprises the Radiolysis Model subroutine within the MPM V2.

3. Sensitivity Results Mixed Potential Model V2.

For anoxic to low oxygen conditions (nano- to micromolar), the fuel dissolution rate predicted by the MPM V2 will depend directly on the concentration of H_2O_2 at the fuel surface. A number of competing processes determine this concentration:

- H_2O_2 is continuously produced within the first 35 μm of the fuel surface. The H_2O_2 concentration depends on dose rate and the generation value G_{H2O2}, which is determined by the Radiolysis Model subroutine based on local $[O_2]$ and $[H_2]$ for a given dose rate.
- H_2O_2 diffuses towards or away from the fuel surface depending on the concentration; the diffusion rates near the surface will be moderated by the corrosion layer.
- H_2O_2 concentration at environmental boundary (3 mm from fuel) is defined to be zero.
- H_2O_2 is consumed (dominantly) at the fuel surface by the following coupled half-reactions:

$$H_2O_2 + 2e^- \rightarrow 2OH^- \quad (2)$$

$$UO_2 \rightarrow UO_2^{2+} + 2e^- \quad (3)$$

- H_2O_2 consumption rate at the fuel surface increases significantly when the NMP-catalyzed hydrogen oxidation reaction is taken into account and $[H_2] \geq$ 1.0E-5 mole/L (Figure 8):

The increase in the rate of H_2O_2 consumption at the fuel surface when NMP-catalyzed hydrogen oxidation is occurring is caused by the kinetic balance of reactions 1, 2 and 3:

$$H_2 + 2OH^- \rightarrow 2H_2O + 2e^- \quad (4)$$

Specifically, the large anodic current associated with the hydrogen oxidation reactions increases the rate of the dominant cathodic reaction involving hydrogen peroxide reduction. This process is shown schematically in Figure 3c. Therefore, hydrogen peroxide is rapidly depleted when enough hydrogen is present at a fuel surface bearing active NMP sites, thereby decreasing the rate of oxidative dissolution (Equation 1). The relative importance of these processes and other chemical and physical effects on the fuel dissolution rate were studied through a series of model sensitivity runs.

Approximately 300 model runs were performed with MPM V2 to determine the relative impacts that different processes, variables and parameters have on the used fuel dissolution rate calculated by the code. Each model run produces an output file consisting of a 100x2000 cell matrix that includes corrosion potentials, reaction current densities, component fluxes, and concentrations of all components at every point in time at every point in space for the specified conditions. These results have been tabulated and key trends identified.

The detailed model output files are important for understanding interactions between the radiolytic, chemical and physical processes included in the code; however, our ultimate interest (what will be provided to the performance assessment model) is the dissolution rate. Therefore,

the output of the MPM V2 sensitivity runs has been synthesized and is represented here in terms of grams of fuel dissolved per surface area per time (Figure 7).

Figure 7 does not explicitly show the time evolution of the variables; however, the direction of the dose rate and temperature arrows are used to indicate that these variables will be decreasing with time as the fuel decays. The pH and temperature effects on the fuel dissolution rate are of about the same magnitude and are indicated by the same arrow.

It is important to note that there are still relatively large uncertainties in the quantification of how the temperature and pH will affect the fuel dissolution rate. For example, the temperature dependence of most reactions in the parameter database (specifically Table 4) is quantified using a reasonable (based on geochemical literature) place holder value of 60,000 J/mole for the activation energy. This, as well as terms accounting for pH dependence and complexation, need to be evaluated experimentally to reduce uncertainties.

Consistent with the experimental literature, the model indicates that decreasing dose rates and temperature decrease the rate of fuel dissolution by almost two orders of magnitude. The main chemical effects included in the model are due to pH and dissolved carbonate, which complexes uranium to increase its dissolved concentration limit. As acidity and carbonate concentrations increase, the fuel dissolution rate increases. The light blue arrows show that fuel dissolution rate decreases with decreasing G_{H2O2} values (due to increasing $[H_2]$ and decreasing $[O_2]$), increasing schoepite corrosion layer thickness, and increasing concentrations of ferrous iron.

All of these effects, however, are minor relative to the fuel-protecting process that involves the oxidation of H_2 at the fuel surface (dark blue arrow in Figure 7). As shown in Figure 3, H_2 is included in the MPM V2 in a catalytic reaction occurring on the NMP surfaces. The amount of hydrogen reacted depends on its concentration and the surface area of the NMP. For the sensitivity runs summarized in Figure 7, a surface coverage of 1% NMP on the fuel surface was used to quantify the H_2 effect for various H_2 concentrations. Results show that presence of 100 bar H_2, which may be expected in repositories at 500 meters depth with steel waste package materials, can essentially shut off the oxidative dissolution of the fuel (SKB, 2011). Radiolytic production of H_2 is sufficient to cause a small decrease in the fuel dissolution rate on the same order as the effects of G_{H2O2} and surface layers, but the anodic corrosion of steel can have a much greater effect.

Figure 8 shows plots from the MPM V2 sensitivity runs that quantify the H_2 effect at two dose rates. The identical shapes indicate that it is the decrease in the fuel corrosion potential caused by the coupling of the H_2 oxidation to the U(IV)/U(VI) couple that is responsible for the dramatic decrease in the fuel dissolution rate with increasing H_2 concentrations (through the reactions shown conceptually in Figure 3). The dissolution rates calculated for H_2 generated from radiolysis and by steel corrosion (values of 1 bar and 10 bars provided to show sensitivity) are indicated in Figure 8a. Figure 8b shows the corrosion potentials from the electrochemical experiments of Broczkowski et al, 2005 for SIMFUELs made with and without added NMP. Those results suggest that the presence of NMP at the fuel surface is largely responsible for the observed H_2 effect, although the effect does occur to a lesser extent in the absence of NMP. An

experimental approach has been designed at ANL to quantify that effect in a future version of the MPM.

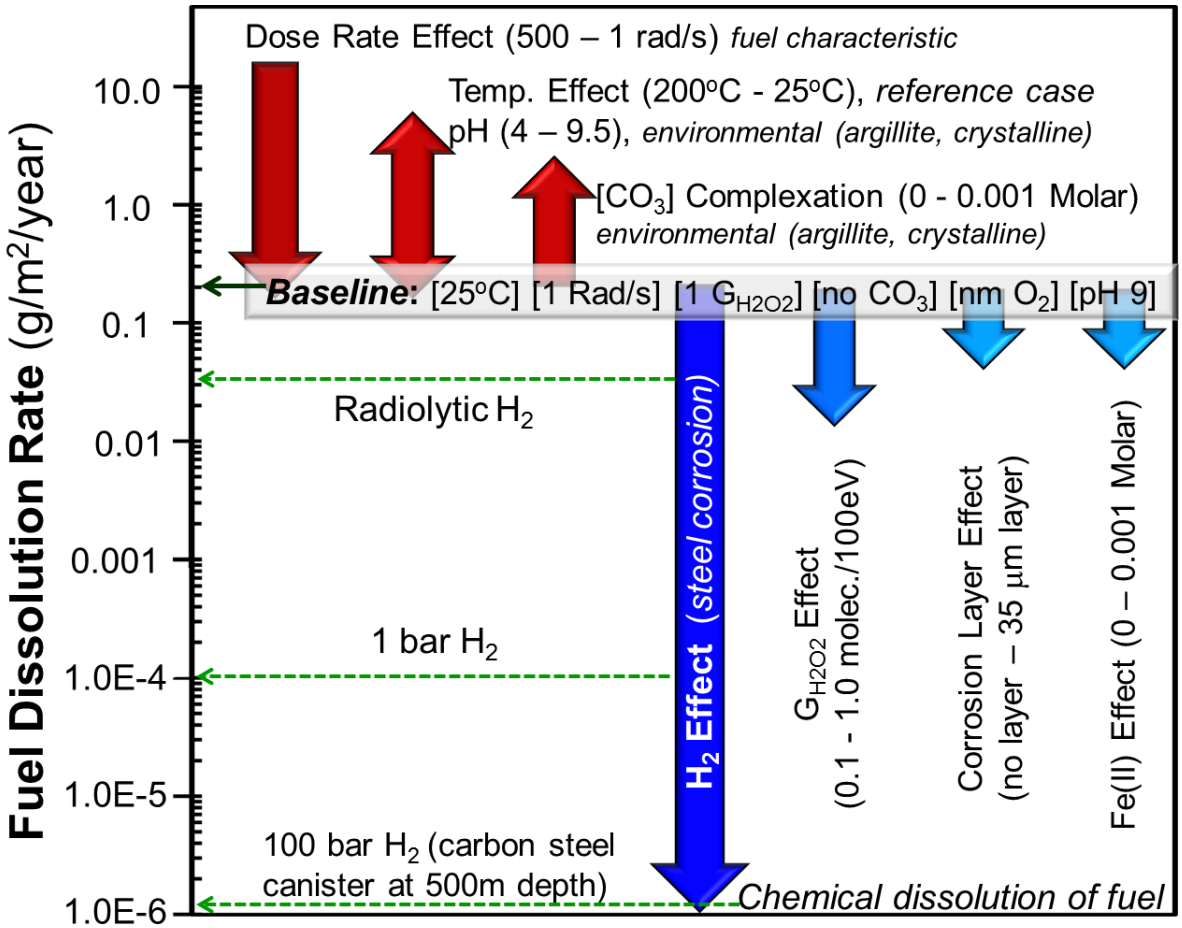

Figure 7. Summary of compiled results from FY2014 MPM V2 sensitivity runs.

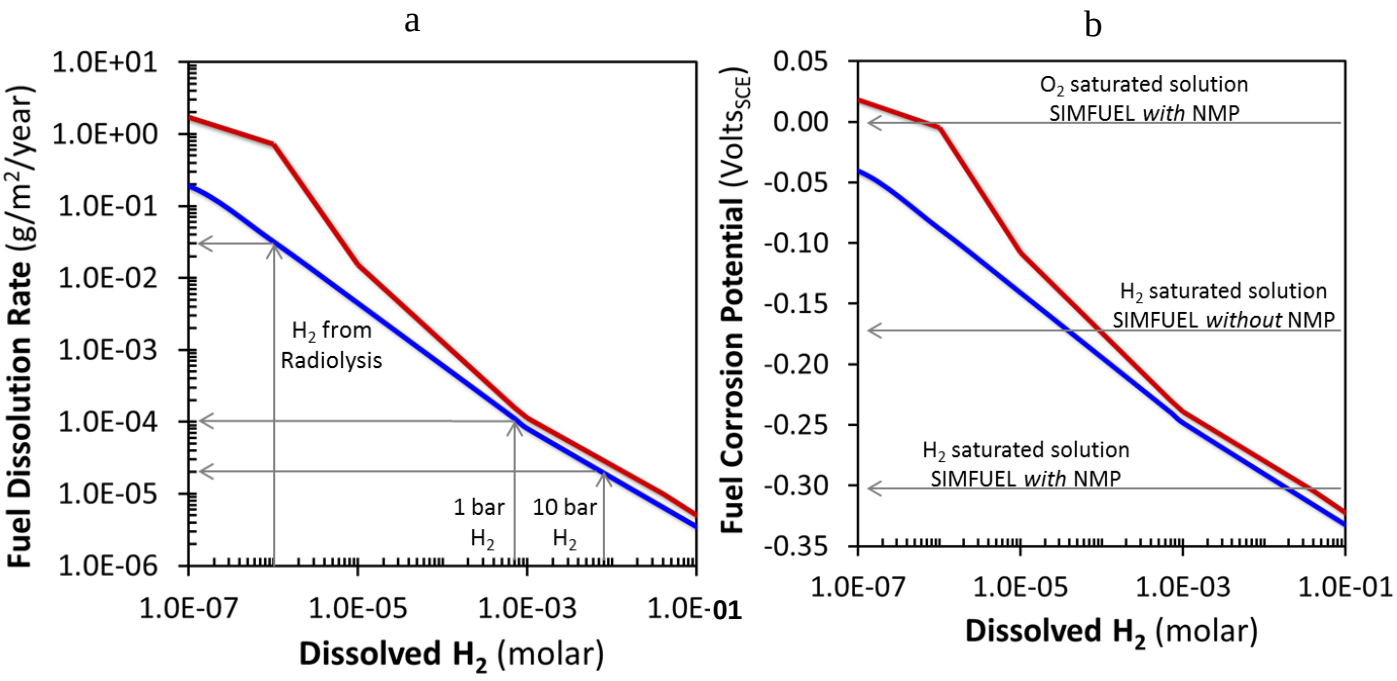

Figure 8. Details of (a) fuel dissolution rate and (b) corrosion potential calculated using MPM V2 for two dose rates (100 rad/s, red and 25 rad/s, blue).

4. Conversion of MPM V2 from MATLAB to Fortran

The MPM was written in MATLAB to utilize available functions (e.g., to solve ordinary differential equations for mass transport) to facilitate the development of additional process modules, such as including catalytic reactions on NMP and a more detailed radiolysis model. The purpose of the language conversion is to facilitate incorporation of the MPM directly into the performance assessment models for argillite and crystalline rock environments. The initial Fortran version of the Argonne MPM will be issued in early FY2015 to serve as a prototype to develop input and output communication links with PA and other process models. Continued development of the MPM, such as including modules for steel corrosion and the degraded NMP catalysis efficiency due to corrosion and poisoning, will be done using MATLAB to quickly evaluate optional approaches and interactions with the rest of the code. The finalized modules will then be translated to Fortran. This development plan is summarized schematically in Figure 1.

The specifics on the conversion are as follows:

- Programming language: Intel(R) Visual Fortran Compiler XE 14
- Additional libraries: LAPACK 3.5.0 Windows 32-bit static library (from http://icl.cs.utk.edu/lapack-for-windows/lapack/#libraries)
- Development environment: Visual Studio 2008

To date, a significant amount of the MPM Fortran code has been written and some internal checks (convergence of individual modules) have been done. Initial meetings with personnel developing the PA model have been scheduled for August and November 2014 to discuss the conceptual approach being taken and the interfaces and information exchanges between the Fortran MPM and PA process models. The following provides an annotated list of issues being addressed in the development of the Fortran MPM to support those discussions.

Inputs to MPM:

- There will be two entry points, one for interaction with the PA model and one for a stand-alone run.
- The input to the MPM is the environmental solution chemistry, temperature and dose rate
  - Currently, the environmental solution information that needs to be passed into the MPM includes the pH and concentrations of dissolved oxygen, hydrogen, iron, and carbonate.
  - It is anticipated that reactions with sulfate, chloride and bromide will be added to the MPM in future versions, so the codes are being set up to allow for expanding the number of components (chemical species).
- There are two types of parameters:
  - System parameters that are used in the PA model and other process models
  - MPM parameters that define characteristics of the mixed potential model only.
- The interface is under development, but it is envisioned that the system parameters will be passed into the MPM while an auxiliary function will read the MPM parameters from a data file.

The MPM parameters will be contained in a user-modifiable text file.

Outputs from MPM:

- There will be two exit points, one for interaction with the PA model and one for a stand-alone run.
    - Output to the PA model will be the fuel dissolution rate (mass/surface area/time) and the final concentrations of all components.
    - Output for the stand-alone model will generate a text data file containing the fuel dissolution rate, the concentrations of components, and calculated electrochemical quantities used to determine the fuel dissolution rate, namely, corrosion potential and reaction current densities.

5. Conclusions and Future Work

The major accomplishments for Argonne's FY2014 work on the Mixed Potential Model (MPM) development project were as follows:

- Added a working noble metal particle (epsilon phase) domain on fuel surface to account for the protective hydrogen effect.
- Incorporated the radiolysis model subroutine in MPM (using an analytical function provided by PNNL)
- Performed systematic sensitivity runs that identify and quantify the processes that affect the fuel dissolution rate.
- Compared sensitivity results with available experimental data (ongoing)
- Developed a research priority list based on results from sensitivity study and comparison with experimental results

The key observation to come out of the MPM sensitivity studies was that the set of coupled electrochemical reactions that comprise the model can be used to quantify the effectiveness of hydrogen within a breached canister to effectively shut down the radiolytic oxidative dissolution of the fuel. At sufficiently high hydrogen concentrations, fuel dissolution will only occur through the much slower chemical dissolution mechanism. This is consistent with experimental results from a number of repository programs (e.g., Shoesmith, 2008; Grambow and others, 2010) and with results from initial electrochemical tests performed in FY2013 as part of this study. The capacity to quantify the hydrogen effect in the used fuel degradation model will provide more realistic radionuclide source terms for use in PA.

The relative effects of temperature, dose rate (burnup), radiolysis, pH, carbonate complexation, ferrous iron and corrosion layer formation were also evaluated in the FY2014 sensitivity runs. All of these variables will influence the fuel degradation rate in distinct ways within argillite and crystalline rock, and other potential disposal environments. However, our sensitivity runs show that the hydrogen effect could be by far (up to four orders of magnitude greater, depending on the hydrogen concentration) the most dominant.

The MPM is uniquely suited to quantify the hydrogen effect on used fuel degradation because it explicitly accounts for all relevant interfacial redox reaction kinetics using fundamental electrochemical principles. This includes the impacts of phases present in the fuel, such as the catalytic effects of noble metal particles and the fuel surface itself, and other materials present in

the disposal system that supply reactants or affect key redox reactions. The anoxic corrosion of steels present in the waste package is the main source of hydrogen in the waste package. The MPM was developed with the initial focus on reactions at the fuel surface, and the dissolved hydrogen concentration is currently a user-input value. To account for the hydrogen effect in long-term model runs, corrosion kinetics of steel components leading to hydrogen generation needs to be incorporated into the model and coupled with fuel dissolution kinetics through the dissolved hydrogen concentration.

The current version of the MPM has proven effective for quantifying key processes affecting the rate of used fuel degradation; however, the implementation of MPM within a performance assessment model requires further model development and focused experimental work to provide data and quantify uncertainties in the existing database used to determine model parameter values representing disposal environments of interest. In order to take advantage of the work that has been done so far on the MPM, a number of needs have been identified:

- Incorporate the kinetics for hydrogen generation during the anoxic corrosion of steels into MPM as the source term for hydrogen.
- Perform focused electrochemical experiments with noble metal particle and lanthanide-doped UO_2 electrodes to determine parameter values needed to accurately model the effects of hydrogen, potential catalytic poisons such as bromide, and the pH and reaction temperature dependencies of fuel dissolution.
- Convert the MPM from MATLAB to Fortran to facilitate integration with PA codes (PFLOTRAN) (ongoing)
- Complete sensitivity runs to identify and assess inputs and outputs for integrating Fortran MPM into PA

6. References

Broczkowski, M. E., Noël, J. J., Shoesmith, D. W., (2005). "The inhibiting effects of hydrogen on the corrosion of uranium dioxide under nuclear waste disposal conditions." *Journal of Nuclear Materials 346,* 16-.

Buck E., Jerden, J., Ebert, W., Wittman, R, (2013). *Coupling the Mixed Potential and Radiolysis Models for Used Fuel Degradation.* FCRD-UFD-2013-000290.

Christensen, H., Sunder, S. (1996). "An evaluation of water layer thickness effective in oxidation of UO_2 fuel due to radiolysis of water." *Journal of Nuclear Materials, 238,* 70-77.

Ebert, W. L., Cruse, T. A., and Jerden J., (2012). *Electrochemical Experiments Supporting Oxide Fuel Corrosion Model*. FCRD-UFD-2012-000201.

R.J. Finch, R.C. Ewing (1992) "The corrosion of uraninite under oxidizing conditions." *Journal of Nuclear Materials, 190,* 133-156.

B. Grambow, J. Bruno, L. Duro, J. Merino, A. Tamayo, C. Martin, G. Pepin, S. Schumacher, O. Smidt, C. Ferry, C. Jegou, J. Quiñones, E. Iglesias, N. Rodriguez Villagra, J. M. Nieto, A. Martínez-Esparza, A. Loida, V. Metz, B. Kienzler, G. Bracke, D. Pellegrini, G. Mathieu, V. Wasselin-Trupin, C. Serres, D. Wegen, M. Jonsson, L. Johnson, K. Lemmens, J. Liu, K. Spahiu, E. Ekeroth, I. Casas, J. de Pablo, C. Watson, P. Robinson, D. Hodgkinson, (2010). *Model Uncertainty for the Mechanism of Dissolution of Spent Fuel in Nuclear Waste Repository*, 2010 Euratom EUR 24597 EN EUROPEAN COMMISSION, Final Report for MICADO project.

E.C. Gaucher, C. Tournassat, F.J. Pearson, P. Blanc, C. Crouzet, C. Lerouge, S. Altmann, 2009, "A Robust Model for Pore-water Chemistry of Clayrock." *Geochimica et Cosmochimica Acta, 73* 6470–6487

Guimerà, J., Duro, L., Delos, A. (2006). *Changes in Groundwater Composition as a Consequence of Deglaciation Implications for performance Assessment*, R-06-105, Swedish Nuclear Fuel and Waste Management Co, SKB, November 2006.

Jerden, J., Frey, K., Cruse, T., and Ebert, W. (2012). *Waste Form Degradation Model Status Report: ANL Mixed Potential Model, Version 1. Archive*. FCRD-UFD-2013-000057.

Jerden, J., Frey, K., Cruse, T., and Ebert, W. (2013). *ANL Mixed Potential Model with Experimental Results: Implementation of Noble Metal Particle Catalysis Module*. FCRD-UFD-2013-000305.

Kerisit, S., Liu, C. (2010). "Molecular simulation of the Diffusion of Uranyl Carbonate Species in Aqueous Solution." *Geochimica et Cosmochimica Acta, 74,* 4937-4952.

King, F. and Kolar, M. (1999) *Mathematical Implementation of the Mixed-Potential Model of Fuel Dissolution Model Version MPM-V1.0,* Ontario Hydro, Nuclear Waste Management Division Report No. 06819-REP-01200-10005 R00.

King, F. and Kolar, M. (2002). *Validation of the Mixed-Potential Model for Used Fuel Dissolution Against Experimental Data*., Ontario Hydro, Nuclear Waste Management Division Report No. 06819-REP-01200-10077-R00.

King, F. and Kolar, M. (2003). *The Mixed-Potential Model for UO2 Dissolution MPM Versions V1.3 and V1.4*., Ontario Hydro, Nuclear Waste Management Division Report No. 06819-REP-01200-10104 R00.

Macpherson, J.V., and Unwin, P.R. (1997). "Determination of the Diffusion Coefficient of Hydrogen in Aqueous Solution Using Single and Double Potential Step Chronoamperometry at a Disk Ultramicroelectrode." *Analytical Chemistry, 69,* 2063-2069.

Murphy, W.M. and Codell, R.C. (1999). *Sci. Basis Nuclear Waste Mgt. XXII, Materials Research Society*, 551-558.

Nielsen and Jonsson, (2006). "Geometrical Alpha- and Beta-dose Distributions and Production Rates of Radiolysis Products in Water in Contact with Spent Nuclear Fuel." *Journal of Nuclear Materials, 359,* 1-7.

Pastina, B. and LaVerne, J. A. (2001). "Effect of Molecular Hydrogen on Hydrogen Peroxide in Water Radiolysis." *Journal of Physical Chemistry A105,* 9316-9322.

Radulescu, (2011), LETTER REPORT, Reactor and Nuclear Systems Division, Repository Science/Criticality Analysis FTOR11UF0334, August, 2011

Shoesmith, D.W., M. Kolar, and F. King (2003). "A Mixed-Potential Model to Predict Fuel (Uranium Dioxide) Corrosion Within a Failed Nuclear Waste Container" *Corrosion, 59*, 802-816.

Shoesmith, D. W. (2008). *The Role of Dissolved Hydrogen on the Corrosion/Dissolution of Spent Nuclear Fuel*, NWMO TR-2008-19, November 2008 Nuclear Waste Management Organization, 22 St. Clair Avenue East, 6th Floor, Toronto, Ontario M4T 2S3, Canada

SKB (Svensk Kämbränslehantering AB [Swedish Nuclear Fuel and Waste Management Company]) 2011. *Long-Term Safety for the Final Repository for Spent Nuclear Fuel at Forsmark*, Technical Report TR-11-01. Three volumes. Stockholm, Sweden: Svensk Kärnbränslehantering AB.

Torrero, M.E., E. Baraj, J. De Pablo, J. Gimenez, and I. Casas (1997). "Kinetics of Corrosion and Dissolution of Uranium Dioxide as a Function of pH." *International Journal of Chemical Kinetics, 29,* 261-267.

Trummer, M., Roth, O., and M. Jonsson, M. (2009). "H_2 Inhibition of Radiation Induced Dissolution of Spent Nuclear Fuel." *Journal of Nuclear Materials, 383,* 226-230

Tsai, H. (2003). "NRC Review of ANL High-Burnup Cladding Performance Program, July 16, 2003".

Uchida, H., Izumi, K., Aoki, K., Watanabe, M., (2009). "Temperature-Dependence of Hydrogen Oxidation Reaction Rates and CO-Tolerance at Carbon-Supported Pt, Pt-Co, and Pt-Ru Catalysts." Phys. Chem. Chem. Phys., 11, 1771-1779

Vinsot A., Mettler S. and Wechner S. (2008). "In situ characterization of the Callovo-Oxfordian pore water composition." Phys.Chem. Earth, 33, S75–S86.

Appendix 1

MATLAB Code for The Radiolysis Mode Subroutine

The analytical function on which this code is based was supplied by Rick Wittman and Edgar Buck of PNNL in early 2014.

```
%************************************************************************
%
% Inputs:
%   rad    = (J/kg)/s
%   cO2    = mol/m^3
%   cH2    = mol/m^3
% Outputs:
%   Gval   =  mol/(J/kg)/m^3
%   dcO2    = (mol/(J/kg)/m^3)/(mol/m^3)
%   dcH2    = (mol/(J/kg)/m^3)/(mol/m^3)
%
%************************************************************************

function [Gval,dcO2,dcH2] = PNNL_gval(rad,cO2,cH2)

  % Constants
  Na     = 6.022e23;     % 1/mol           (Avogadro's constant)
  eV     = 1.602e-19;    % J/eV            (Elementary charge)
  mwH2O  = 0.018;        % kg/mol          (Molecular weight of water)

  % Parameters
  hH2     = 7.8e-1;       % mol/bar/m^3     (Henry's law constant: H2)
  penD    = 3.5e-5;       % m               (Alpha penetration depth)
 % DO2     = 1.7e-9;
  DO2    = 2.5e-9;       % m^2/s           (Diffusivity: O2)
 % DH2O2   = 1.7e-9;
  DH2O2  = 1.9e-9;       % m^2/s           (Diffusivity: H2O2)
  rhoH2O  = 1e3;          % kg/m^3          (Groundwater density)

  % Rate constants
  rk27 = 2.1e7;          % m^3/mol/s
  rk23 = 1.1e-2/56;      % m^3/mol/s
  rk26 = 9.0e4;          % m^3/mol/s

  % Equilibrium constants
  ratk1 = rk26/rk27;
  ratk2 = rk27/rk23;

  % Intermediate quantities
  presH2  = cH2/hH2;         % bar
  concH2O = rhoH2O/mwH2O;    % mol/m^3
  dpH2dH  = 1/hH2;           % bar/(mol/m^3)

  % G-values
  GH     = 0.10*(1-exp(-presH2/0.1));        %  molecule/100eV
  GOH    = 0.35*(1-exp(-presH2/0.3));        %  molecule/100eV
  dGHdH  =          exp(-presH2/0.1)*dpH2dH; % (molecule/100eV)/(mol/m^3)
```

```
  dGOHdH = 0.35/0.3*exp(-presH2/0.3)*dpH2dH; % (molecule/100eV)/(mol/m^3)

  % Other
  dN       = 4.75e-3/penD;                              %  m/m
  v1       = ratk2/concH2O;                             %  m^3/mol
  dlam0    = v1*rhoH2O/eV/Na*rad.*(GH+GOH)/1e2;         %  1/s
  dk       = DO2/penD^2;                                %  1/s
  dkH2O2   = DH2O2/penD^2;                              %  1/s
  ddlam0dH = v1*rhoH2O/eV/Na*rad.*(dGHdH+dGOHdH)/1e2; % (1/s)/(mol/m^3)

  B    = cO2*v1 - dN*dlam0/dk - 1;
  dBdO = v1;
  dBdH = -dN*ddlam0dH/dk;

  X    = 0.5*(B+sqrt(B.*B-4*cO2));
  dXdO = 0.5*(dBdO+0.5*(2*B.*dBdO-8*cO2)./sqrt(B.*B-4*cO2));
  dXdH = 0.5*(dBdH+0.5*(2*B.*dBdH      )./sqrt(B.*B-4*cO2));

  dlam    =  dlam0./(1+X);              %  1/s
  ddlamdO = -dlam0.*dXdO./(1+X).^2;     % (1/s)/(mol/m^3)
  ddlamdH = -dlam0.*dXdH./(1+X).^2;     % (1/s)/(mol/m^3)

  % Results
  dNom = (dkH2O2 + ratk1*dN*dlam);
  Gval =  dkH2O2./dNom;                          %  molecule/100eV
  Gval =  Gval*rhoH2O/Na/eV/1e2;                 %  mol/(J/kg)/m^3

  dcO2 = -dkH2O2*(ratk1*dN*ddlamdO)./dNom.^2;   % (molecule/100eV)/(mol/m^3)
  dcO2 =  dcO2*rhoH2O/Na/eV/1e2;                % (mol/(J/kg)/m^3)/(mol/m^3)

  dcH2 = -dkH2O2*(ratk1*dN*ddlamdH)./dNom.^2;   % (molecule/100eV)/(mol/m^3)
  dcH2 =  dcH2*rhoH2O/Na/eV/1e2;                % (mol/(J/kg)/m^3)/(mol/m^3)

  return

end

%**************************************************************************


%**************************************************************************
```